Assessment of chemical and mechanical behavior of bamboo pulp and nanofibrillated cellulose exposed to alkaline environments

Viviane da Costa Correia[1*], Mònica Ardanuy[2], Josep Claramunt[3], Holmer Savastano Junior[1]

[1]*University of São Paulo (USP), Department of Biosystems Engineering, Research Nucleus on Materials for Biosystems, Pirassununga, SP, Brazil.*

[2]*Universitat Politècnica de Catalunya (UPC), Department of Materials Science and Metallurgy, Terrassa, Barcelona, Spain.*

[3]*Universitat Politècnica de Catalunya (UPC), Department of Agri-Food Engineering and Biotechnology, Castelldefels, Barcelona, Spain.*

*Corresponding author: vivianecostcor@usp.br

Phone number: +55 19 3565-4176

Abstract

This study was performed to study the effects of the cement paste composition (calcium aluminate cement -CAC- and a geopolymer in comparison to Portland cement -OPC-) on bamboo pulp and nanofibrillated cellulose (NFC). The changes in the composition and chemical structure of the fibers were analyzed by X-ray photoelectron spectroscopy (XPS) and Fourier-transform infrared spectroscopy (FTIR). The changes in the mechanical strength were evaluated through tensile tests on the fibers after immersion on the cement pastes, in the form of sheets. The XPS results showed that the immersion of the pulp and NFC in the different pastes (CAC, geopolymer and OPC) modified the chemical surface of these fibers: it was found removal of lignin and extractives and some degradation of hemicellulose and cellulose. The FTIR analysis indicated modifications in the hydrogen bonds energy. The tensile strength of pulp sheets decreased in 70% and 34% after immersion in OPC and geopolymer, respectively. The tensile strength of the NFC sheets decreased 36%, 68% and 54% after immersion in OPC, CAC and geopolymer, respectively. Thus, the response of the bamboo pulp and NFC immersed in different cement pastes was different due the inherent characteristics of such fibers, and not only the Portland cement should be considered as harmful to lignocellulosic fibers. Although CAC and geopolymer are free of calcium hydroxide, the high alkalinity of these pastes also accelerated the degradation process of lignocellulosic fibers.

Keywords: bamboo pulp, nanofibrillated cellulose, degradation, high alkalinity

1. Introduction

Fiber-cement composites are construction building materials that can be used in applications such as sidings, roofing and ceiling panels. These materials are basically composed of Ordinary Portland cement (OPC), limestone, cellulosic pulp and synthetic fibers, like polypropylene, and polyvinyl alcohol. In the Hatschek process cellulosic pulps are used as processing fiber. In this process the pulps are responsible for the retention of particles in the cementitious matrix and to facilitate the water removal during the drainage stage of the production process. In addition, the pulp is also a reinforcing component in the micrometric scale of fiber-cement (Bentur and Mindess 2007).

Other form of cellulosic fibers with potential to use as reinforcement of cement-based materials is nanofibrillated cellulose (NFC). NFC is produced by mechanical disintegration without chemicals or even biological process. It is described as a long and flexible cellulosic nano-material, which is obtained from cellulose fibers that have been fibrillated to achieve agglomerates of cellulose microfibril units (Missoum et al. 2013). NFCs contain crystalline and amorphous regions and they have diameters in the range of 5–60 nm and lengths of several hundred nanometers (Klemm et al. 2011; Klemm et al. 2018). NFCs have high specific surface area, which increase the interaction of the fibers with the matrix promoting the higher mechanical strength of the reinforced composites (Correia et al. 2018a; Correia et al. 2016; Ardanuy et al. 2012a; Ardanuy et al. 2012b). According to Correia et al. (2018b) NFC contribute to the increase of the physical and chemical adhesion, friction and mechanical anchorage with the matrix with respect pulps, induced by its high specific surface area.

Eucalyptus and pinus pulp are traditionally used in the producing of commercial fiber-cement products by the Hatschek process, but some studies have shown that bamboo pulp and NFCs also have potential to be used as reinforcement for these cement-based materials (Correia et al. 2018a ; Li et al. 2017; Xie et al. 2015; Correia et al. 2014; Rodrigues et al. 2010; Rodrigues et al. 2006; Coutts and Ni 1995).

The drawback of the use of lignocellulosic fibers in cementitious matrices based on OPC is their low durability in this environment. The high alkalinity (pH ≈ 13) and the presence of

calcium hydroxide in the pore solution of OPC affect the durability of cellulosic fibers (Cheng et al. 2018; Wei 2018; Wei and Meyer 2015; Tolêdo Filho et al. 2003).

The high alkalinity of water in the pore of the cementitious matrix dissolves the lignin and hemicelluloses of fiber; alkaline hydrolysis of cellulose molecules leads to degradation of molecular chains and the reduction in the degree of polymerization and lower tensile strength; crystallization of calcium hydroxide in the lumen, walls of the individual fibers and middle lamella leads to a decrease in the fiber flexibility and mechanical strength (Singh 1985; Gram 1988; Tolêdo Filho et al. 2000; Mohr et al. 2005; Wei and Meyer 2017). Thereby, the degraded lignocelulosic fibers can decrease the durability of the material and consequently lead it to premature failure (Wei and Meyer 2017).

The use of cellulosic pulp as reinforcement of cement-based materials is a way to mitigate the degradation because the high alkalinity of cementitous matrix deteriorates the lignin and hemicellulose, and in chemical pulping processes most part of these components is removed. Other measures to reduce fiber degradation and increase the durability of composites include the use of calcium hydroxide free cementitious matrices or the use of supplementary cementitious materials as a partial replacement of OPC (Tolêdo Filho et al. 2003; Mohr et al. 2007) and the use of accelerated carbonation curing (Almeida et al. 2013; Santos et al. 2015). According to Mármol and Savastano (2017), these measures aim to reduce the level of calcium hydroxide in cement matrices.

Gram (1988) studied the durability of sisal fibers in matrix with high alumina cement and concluded that the use of these cements significantly minimize the degradation of composite subjected to accelerated aging. In this study the author observed that after the alternating of 120 cycles of immersion and drying, the post-cracking peak strength of composite with high alumina cement decreased by 56.2% in comparison to 98.8% for the OPC matrix. According to Mohr et al. (2007) this is due the consumption of calcium and aluminate ions from the pore solution that decreases the amount of calcium hydroxide and secondary ettringite reprecipitation.

Claramunt et al. (2018) evaluated the mechanical behavior of calcium aluminate cement (CAC) composites reinforced with flax's nonwoven fabrics, and the durability of the composites subjected to five cycles of immersion and drying. The authors found that the CAC matrix is effective for mitigating the degradation of the fibers after accelerated aging. These results are in accordance with Mohr et al. (2005), who reported that CAC is an alternative to supplementary

cementitious materials and should be evaluated for their respective effect on the progression of degradation of pulp in the fiber-cement composite.

Another promising matrix rich in aluminates and free of calcium hydroxide is the geopolymer. Among the advantages of the use of geopolymers as an inorganic matrix is that this matrix is considered eco-friendly. The cure of geopolymers is generally performed at room temperature and, therefore, its synthesis requires less energy, and depending on the activator there is a reduction of up to 80% CO_2 compared to OPC (Tailby and MacKenzie 2010; Villa et al. 2010; Firdous et al. 2018).

Due to fragile behavior of geopolymer, the use of vegetal fibers as reinforcement of this matrix has been studied (Alomayri et al. 2013; 2014; Chen et al. 2014; Assaedi et al. 2015). However, as the high alkalinity of the geopolymer can be harmful to the lignocellulosic fibers, Yan et al. (2016) suggest the composition of the geopolymer with high content of fly ash, blast-furnace slag, metakaolin and silica. But there are no studies to confirm the increased durability of the fibers and geopolymer composites with the adoption of these measures.

Thus, this study aims assess the chemical and mechanical degradation of bamboo pulp and nanofibrillated cellulose when exposed to three different highly alkaline unhardened cement pastes (Portland cement, calcium aluminate cement and geopolymer) up to 28 days of age, what can be considered a very severe degradation test.

2. Experimental procedure

2.1 Preparation and characterization of the fibers

Unbleached pulp and nanofibrillated cellulose (NFC) from bamboo were used in this study. The pulp was produced by the organosolv pulping process using a batch reactor. The NFC was produced from bamboo pulp using the grinding method. The parameters used for the pulping and nanofibrillation, as well as their characterization are described in Correia et al. (2016). The chemical, physical and morphological characteristics of the fibers are presented in Table 1.

155 Table 1 – Chemical, morphological and physical characteristics of the pulp and NFC

Chemical composition		
Components (%)	Pulp	NFC
Extractives	6.92 ± 1.47	9.07 ± 1.25
Lignin	9.85 ± 3.86	9.67 ± 2.37
Holocellulose	85.39 ± 1.42	85.28 ± 1.96
Cellulose	82.75 ± 0.42	77.82 ± 1.02
Hemicellulose	2.64 ± 0.42	7.46 ± 1.02
Morphological and physical characteristics		
Average diameter	(2.72 ± 2.64) µm	(13.88 ± 9.47) nm
Density (g/cm^3)	1.51	1.42

156

157 The micrographs obtained via Scanning Transmission Electron Microscopy (STEM) (FEI
158 Magellan 400 L Scanning Electron Microscope) are presented in Figure 1. The images show the
159 difference between pulp and NFC related to their morphology and specific surface area. In this
160 way, considering the difference in the levels of some chemical components (extractives, cellulose
161 and hemicelluloses) and in the morphology is possible to presume that the response of these fibers
162 immersed in different alkaline environment will not be the same.

163 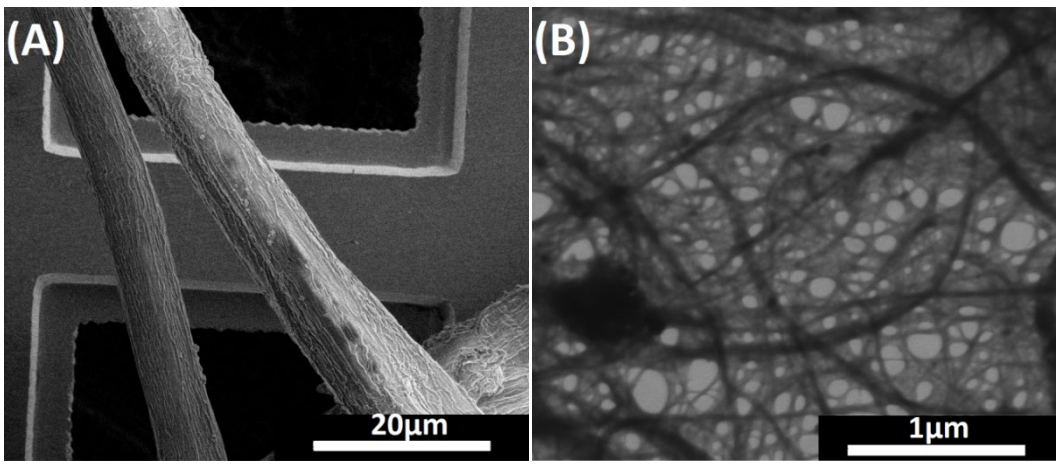

164 Figure 1 – Micrographs of unbleached bamboo pulp (A) and NFC (B) used in the degradation
165 study

166

2.2 Composition of the alkaline pastes

In order to analyze the degradation of the fibers in different alkaline environments, samples of pulp and NFC were prepared in packets, which were produced using a first layer of paper filter and other layer of fabric material. Then, the packets with fibers were immersed in three containers containing the unhardened pastes: Ordinary Portland Cement (OPC) CEM I 52.5 R (EN 197-1: 2011 Standard); Calcium Aluminate Cement (CAC) (EN 14647 Standard), both with a water:cement ratio of 2:1; and geopolymer. The OPC and CAC were supplied by Molins industrial, *Molins de Rei*, Barcelona, Spain. The geopolymer was produced using metakaolin as aluminosilicate source. The activator solution for geopolymerization was made by mixing sodium hydroxide (10M) with silica fume. The metakaolin and silica fume were supplied by Arciresa, Gijón, Asturias, Spain. The molar ratios used were Si/Al = 1.72, Na/Al = 1.01, and H_2O/Na_2O = 11.25.

The objective of this methodology was keeping the fibers in a high alkaline environment, and in contact with the ions of the unhardened cementitious pastes, without direct contact between fibers and mineral particles. After immersion of the packets with fibers in the cement pastes, it was intermittently stirred during 7 days at 1000 rpm to avoid cements hardening. In order to monitor the evolution of the alkalinity of unhardened pastes up to 28 days, which is very severe condition that the fibers were exposed, the pH of the pastes was measured using a bench top pH meter at different ages (0 h, 6 h, 7 days and 28 days). The packets were kept within unhardened pastes for 28 days.

The chemical composition (%wt of oxides) of the OPC, CAC and mineral particles of geopolymer (metakaolin and silica fume) was analyzed by X-ray Fluorescence Spectrometry, and the results are presented in Table 2.

197 Table 2. Chemical composition (%wt of oxides) of Portland cement (OPC), calcium aluminate
198 cement (CAC), metakaolin and silica fume

Oxides (%)	OPC	CAC	Metakaolin	Silica fume
SiO_2	19.26	3.7	54.61	93.5
Al_2O_3	4.02	41.5	40.24	0.32
CaO	57.32	38.1	0.1	0.39
MgO	5.04	0.43	-	0.2
SO_3	3.62	0.01	-	0.03
Na_2O	0.14	0.14	-	0.23
K_2O	1.15	0.02	0.51	0.28
TiO_2	-	1.72	0.13	-
MnO	-	0.01	-	-
Fe_2O_3	3.91	13.20	0.52	0.11
Loss on ignition	2.98	1.41	0.07	3.44

199

200 The heat of hydration of the matrices based in OPC, CAC and geopolymer were
201 determinated using the calorimetry test. The pastes with a water/cement relation of 0.5 were mixed
202 during 5 min at temperature of 25 °C, and then they were placed in glass cylinders. The sealed
203 samples were placed in the calorimeter, which recorded the heat of hydration and reaction during
204 24 h. Figure 2 shows the heat of hydration of OPC and CAC and the heat of reaction of
205 geopolymer.

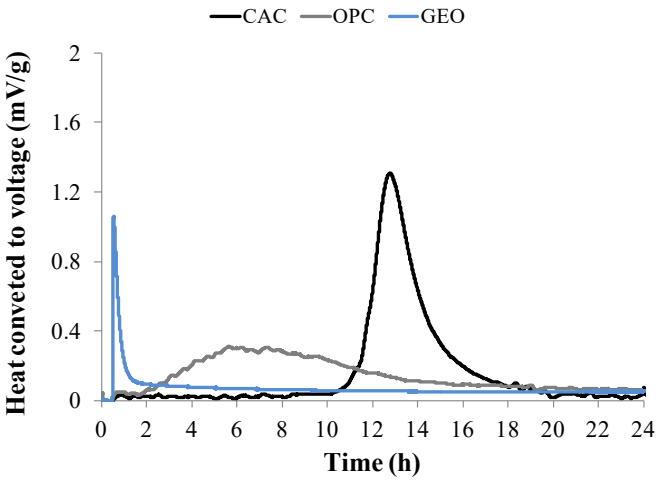

206

207 Figure 2 - Curves of the heat of hydration of OPC, CAC and reaction of geopolymer

2.3 Study of fibers degradation

Sheets of pulp and NFC immersed in the unhardened pastes with OPC, CAC and geopolymer at 28 days were produced for further characterization and analysis of fibers degradation. The sheets of 0.05 mm of thickness were produced by the vacuum filtration from the fibers suspension with 0.2% consistency (by mass). The suspensions were stirred in a laboratory mixer during 5 min and then, they were filtered using hydrophilic polyether sulfone membranes with 90 mm of diameter and pores of 0.1 μm of thickness. After filtration, the sheets were removed from the membrane and then they were oven dried at 60 °C for 48 h. Figure 3 presents the sheets of pulp and NFC that were immersed in alkaline envinronments.

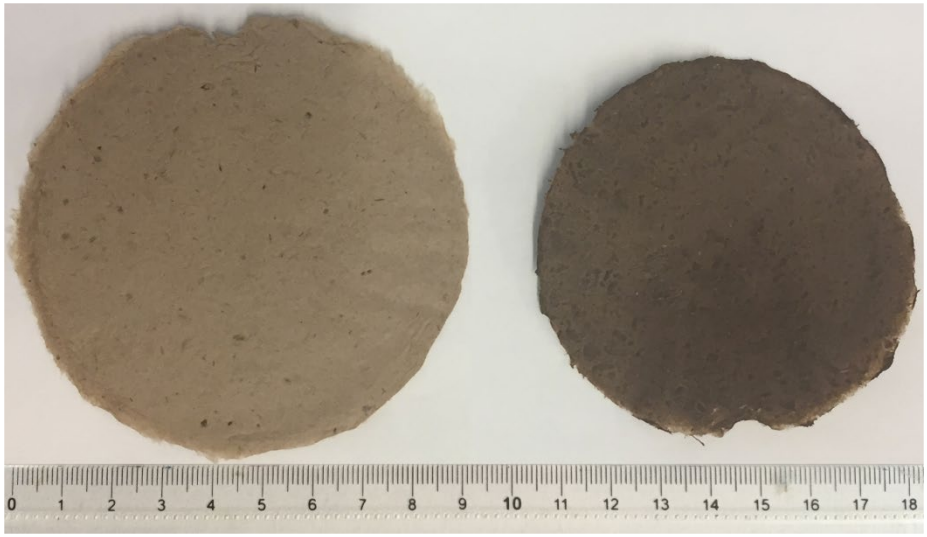

Figure 3– Sheets of pulp (left) and NFC (right) produced after immersion in the alkaline environment

The changes in the chemical structure of the fibers before and after the accelerated degradation test, from immersion of the pulp and NFC in the three alkaline pastes, were analyzed by the X-ray photoelectron spectroscopy (XPS) and Fourier-transform infrared (FTIR) spectroscopy.

The XPS measurements were performed using a SPECS system equipped with Al anode XR50 source operating at 150 W and 12 kV and a Phoibos 150 MCD-9 detector. Samples were placed in a vacuum chamber ($5.0x10^{-8}$ mbar). Survey spectra were recorded in 0.1s/step, 0.5eV /step and 5 scans. The high-resolution were recorded in 0.5 s/step, 0.05eV/step and 3 scans.

Spectra were analyzed using SPECS Prodigy and data processing were performed with CasaXPS software.

The FTIR spectra of pulp and NFC were recorded using a Thermo Scientific Nicolet 6700 FTIR instrument equipped with an Attenuated Total Reflectance (ATR) Smart Orbit Diamond accessory that allows collection of FTIR spectra directly on a sample. The spectra were obtained over the scan range of 4000–600 cm^{-1}, with a spectral resolution of 4 cm^{-1}, and with a total accumulation of 32 scans. Curve fitting for the peak deconvolution was performed by OriginPro 2018 software. The true shape of the peaks obtained from the absorption bands for samples was assumed to be Lorentzian. The number of peaks involved was determined in the range of 2700-3800 cm^{-1}.

The energy of the hydrogen bonds was calculated using the Equation 1 (Poletto et al. 2014; Popescu et al. 2007):

$$E_{H=} \frac{1}{k}\left[\frac{v_0 - v}{v_0}\right] \quad (1)$$

Where ν_0 is the standard frequency corresponding to free OH groups (3650 cm^{-1}), ν is the frequency of the bonded OH groups, and k is a constant ($1/k = 2.625 \times 10^2$ kJ).

The sheets produced for the mechanical characterization were cut in specimens with approximately 30 mm of length and 5 mm of width. For each type of cementitious paste, 22 specimens of NFC and 28 specimens of pulp were produced for the mechanical test. The specimens were subjected to tensile testing using a texture analyser model TA XT Plus with a load cell of 5 N, the cross head speed of 0.1 mm/s and with the gage length of 10 mm.

A statistical analysis was carried out for comparison the tensile strength of fibers immersed in OPC, CAC and geopolymer with the control. The statistical analysis was performed using Statistica software (version 13.4.0.14). After the analysis of ANOVA assumption, an assessment was defined by completely randomized design (CRD) and a comparison between the average values by Tukey test at 5% significance level.

3. Results and discussions

The pH values of the unhardened cementitious pastes at different ages are presented in Table 3. The slight increase in pH of the OPC and CAC pastes over time was observed. This is due the dissolution of minerals and continuous cement hydration reactions, which forms new hydration products with water (Šiler et al. 2016).

Sodium hydroxide is commonly used as alkaline activator of the silicon and aluminum for the geopolymer synthesis. The use of hydroxides and alkali silicates with pH values higher than 13 allows transforming glassy structure partially or totally into a very compacted composite (Khale and Chaudhary 2007). The apparent reduction of the pH of the geopolymer, especially in 6 h, may indicate the dissolution of the silicate and the aluminate and the polymerization of the material, since the gain of 70% strength of the geopolymer occurs in the 3-4 h of cure (Khale and Chaudhary 2007).

The results show that despite the changes occurred in the pH of the pastes over the 28 days, such matrices remained highly alkaline.

Table 3 – pH evolution over time of OPC, CAC and geopolymer

Age \ Cement	OPC	CAC	Geopolymer
0 h	12.95	11.81	13.37
6 h	12.96	11.86	12.84
7 days	13.05	12.46	12.75
28 days	13.16	12.45	12.44

The analysis of the fibers by XPS allowed the evaluation of the effect of the fibers immersion in different unhardened cement pastes and the changes in the composition and chemical structure of the fibers surface. The chemical composition found on the surface of the fibers is shown in Table 4.

Table 4 shows that more than 90% of the fibers surfaces are composed for carbon and oxygen. Besides carbon and oxygen, low amount of nitrogen and calcium was found on the surface

of the fibers. The higher content of calcium is observed, especially, in the fibers (pulp and NFC) immersed in the OPC paste and in the pulp immersed in the CAC paste, in comparison to the control fibers. This is due to the residual calcium ions existing in these cementitious pastes, which migrated to the surface of the fibers. The study of the chemical components on the surface of the fibers is commonly carried out from the oxygen to carbon (O/C) ratio and determination of the non-oxygenated carbons in the high resolution spectrum C1s (Johansson et al. 2005).

Table 4 – Chemical composition and O/C ratio of pulp and NFC surfaces

	Fiber	Chemical elements				
		% C	% O	% N	% Ca	O/C
Control	Pulp	72.12 ± 1.30	26.89 ± 1.19	0.70 ± 0.11	0.29 ± 0.03	0.37 ± 0.02
	NFC	71.81 ± 0.33	27.12 ± 0.82	0.66 ± 0.04	0.41 ± 0.05	0.38 ± 0.01
OPC	Pulp	70.33 ± 1.27	28.21 ± 1.25	0.96 ± 0.15	0.51 ± 0.05	0.40 ± 0.01
	NFC	72.96 ± 0.25	25.71 ± 0.70	0.64 ± 0.02	0.69 ± 0.08	0.35 ± 0.01
CAC	Pulp	69.59 ± 1.45	29.21 ± 1.30	0.79 ± 0.12	0.41 ± 0.04	0.42 ± 0.02
	NFC	70.01 ± 0.32	29.08 ± 0.89	0.55 ± 0.03	0.36 ± 0.04	0.41 ± 0.01
Geopolymer	Pulp	69.96 ± 1.36	28.93 ± 1.34	0.84 ± 0.09	0.26 ± 0.02	0.41 ± 0.02
	NFC	70.96 ± 0.42	28.06 ± 0.86	0.58 ± 0.01	0.39 ± 0.05	0.39 ± 0.01

The O/C ratio is commonly used for the estimation of fibers surface coverage by lignin, and this is possible based on the theoretical O/C ratios of cellulose and lignin, which are 0.83 and 0.33 respectively (Laine et al. 1994). The results of the chemical composition (Table 1) show that after nanofibrillation the fibers are composed of about 9% residual lignin, which is confirmed by the O/C ratio of pulp and NFC control (Table 4). The O/C ratio of all fibers in different conditions is inferior to 0.83 and close to the O/C ratio of lignin.

Moreover, the results show that the immersion of the pulp and NFC in the different environments modified the chemical surface of these fibers. According to Hua et al. (1993), the higher O/C ratio represents the lower amount of lignin and extractives on the surface of the fiber. Thus, the immersion of the pulp in the pastes containing OPC, CAC and geopolymer caused the removal of lignin and extractives from the surface of the fibers.

302 Regarding to NFC, the increase in the O/C ratio of the fibers immersed in CAC paste and
303 geopolymer was also observed, indicating the removal of lignin and extractives. However, the O/C
304 ratio of NFC immersed in OPC was reduced, indicating a higher amount of lignin on the surface of
305 this fiber. According to George et al. (2015) the degradation of hemicelluloses and removal of
306 extractives of the fibers results in lignin exposure, and consequently the reduction in O/C ratio.
307 The modification of the chemical composition of the fibers immersed in OPC, CAC and
308 geopolymer confirms what Wei and Meyer (2017) and Chakar and Ragauskas (2004) reported.
309 According to the authors the high alkalinity environment causes depolymerization and
310 fragmentation of lignin. This fragmentation leads to the generation of free phenolic hydroxyl
311 groups, and in turn the lignin fragments are rendered water/alkali soluble. Similar with
312 lignin, hemicelluloses also experience alkaline attacks and can be converted into fermentable
313 sugar. Thus, lignin acts as a barrier, being the first pulp component to suffer alkaline attack (Mohr
314 et al. 2005 ; Mohr et al. 2006).
315 High-resolution XPS spectra, which give details of the peak C1s, allow the quantitative
316 and qualitative evaluation of the functional groups in the surface of the fibers from decomposition
317 of the C1s peak in carbon atoms (C1, C2, C3, C4). According to Fuentes et al. (2013) and
318 Migneault et al. (2015), the carbon C1 corresponds to the functional groups C-C and C-H; the C2
319 corresponds to C-O-C and C-OH; the C3 corresponds to C=O and O-C-O; the C4 corresponds to
320 O-C=O. The C1 and C4 components arise mainly from lignin and extractives and C2 and C3
321 components arise mainly from hemicelluloses and cellulose (Hua et al. 1993).
322 The results of the deconvolution of peaks C1s of the pulp and NFC immersed in the
323 different highly alkaline and unhardened cement pastes are presented in Figure 4. Figure 4
324 indicates the existence of the four carbon atoms, C1, C2, C3, C4, for the fibers under all
325 conditions. However, Table 5 shows that the proportion of the atoms and functional groups differs
326 for the pulp and NFC immersed in the different pastes.

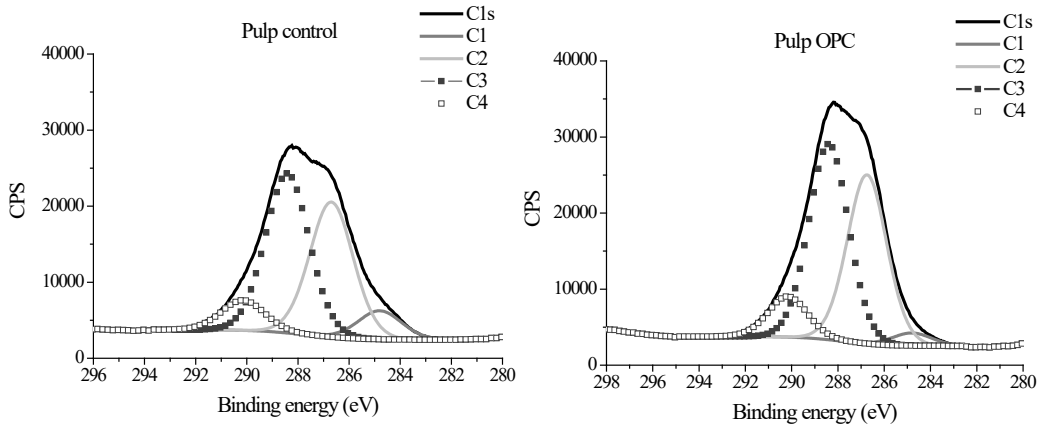

327

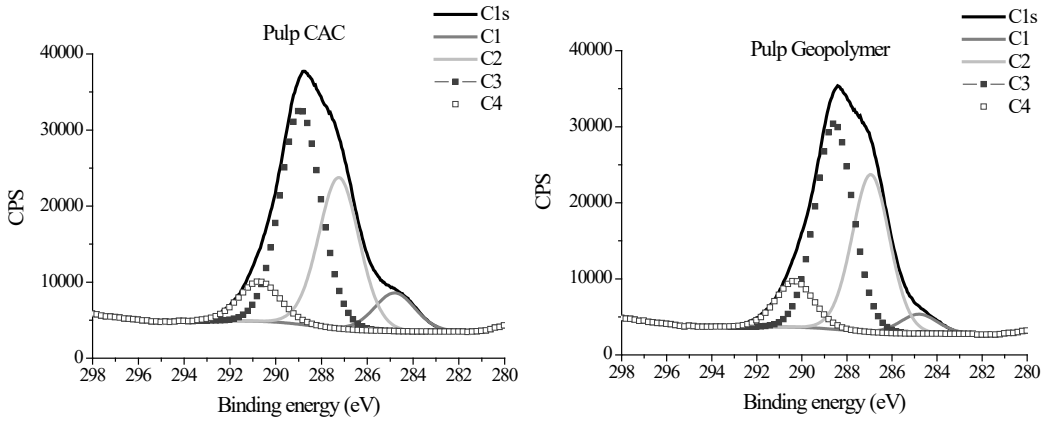

328

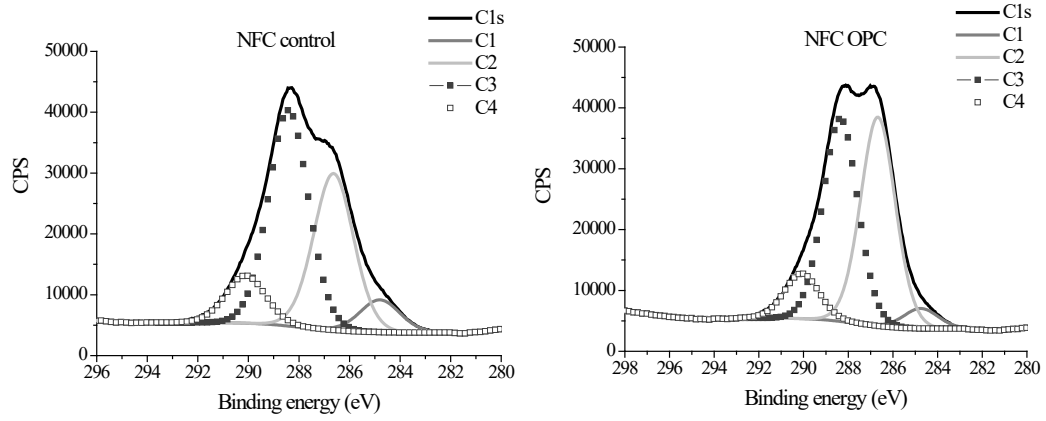

329

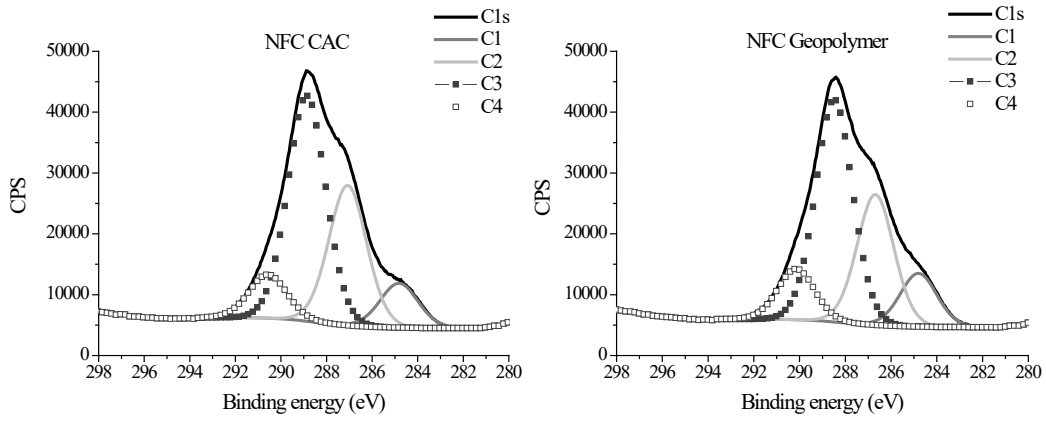

330

Figure 4 – High resolution XPS scan of C1s region for pulp and NFC immersed in unhardened cementitious pastes based in OPC, CAC and geopolymer

Table 5 shows that the main modifications occurred in the components C1 and C2 of the pulp and NFC after the immersion in the different alkaline environments, in comparison to the control. In addition, these components are the main ones for the analysis of lignin and cellulose on the surface of the fibers. According to Johansson (2002) the C-C component in C1 spectrum, originating from carbon atoms that have no oxygen neighbors is due to lignin only, but with the presence of extractives, indicated by the C-H bonds. Thus, Johansson (2002) recommends that the quantification of lignin be based on the C-C percentages. For pure cellulose a large contribution of C2 (83%), and a small contribution of C3 (17%) carbons in the C(1s) peak is expected (Hua et al., 1993; Holmberg et al., 1997; Bastidas et al. 2005). This indicates that the C2 component represents much more cellulose, although the hemicellulose has a similar carbon bond structure to cellulose, that is, all the carbons in hemicellulose are linked to at least one oxygen (Hua et al. 1993). However, hemicellulose has carbonyl groups (C = O), which are strongly present in the C3 and C4 components. In addition, the carbonyl groups are in hemicellulose, lignin and extractives (Bouafif et al. 2008), and this makes the C3 and C4 more heterogeneous and complex.

The results show the reduction of 61% and 44% of carbon C1 in the pulps immersed in OPC and geopolymer respectively, and the increase of 6% of C1 in the pulp immersed in CAC. In the NFC, it is observed that the immersion of these fibers in OPC paste led to a reduction of 40% of C1 and increase of 38% and 63% of C1 in the fibers immersed in CAC and geopolymer, respectively. The reduction of carbon C1 indicates removal of lignin, or extractives, or both, from the surface of the fibers. The increase in C1 indicates the degradation of hemicelluloses or cellulose, leading to exposure of the lignin or extractives on the surface of the fibers. This correlation is clear when considering the reduction of 11% and 18% of the carbon C2 on the surface of NFC immersed in CAC and geopolymer, respectively; and the increase of 27% of C2 on the surface of NFC in OPC. In the pulp, there was a reduction of 11% of C2 for immersion in CAC and the increase of 6% of C2 in the pulp immersed in OPC.

Table 5 – Functional groups on the fibers surface

Fibers	Functional groups			
	% C1 (C-C, C-H)	% C2 (C-O, C-OH)	% C3 (C=O, O-C-O)	% C4 (O-C=O)
Pulp control	8.09 ± 0.58	38.21 ± 0.91	45.18 ± 1.65	8.52 ± 0.88
Pulp OPC	3.05 ± 0.81	40.38 ± 1.01	46.87 ± 1.05	9.70 ± 0.51
Pulp CAC	8.60 ± 0.83	34.06 ± 1.89	48.36 ± 0.99	8.98 ± 1.10
Pulp geopolymer	4.52 ± 1.04	36.73 ± 1.11	47.97 ± 0.52	10.77 ± 1.26
NFC control	7.14 ± 0.97	34.60 ± 2.46	47.72 ± 1.77	10.54 ± 1.73
NFC OPC	4.19 ± 1.11	43.76 ± 1.60	42.59 ± 2.13	9.45 ± 0.47
NFC CAC	9.78 ± 0.94	30.85 ± 1.62	49.76 ± 1.49	9.60 ± 0.83
NFC geopolymer	11.65 ± 1.38	28.55 ± 1.44	48.70 ± 1.34	11.10 ± 0.55

These results of the high-resolution XPS spectra confirm the low resistance of lignin, especially in pastes based on OPC and geopolymer. This reinforces the assertion that the high alkalinity dissolves the lignin and hemicelluloses of fiber, and besides the low durability of these components in a highly alkaline environment, they are sensitive to $Ca(OH)_2$, present in the OPC matrix. About the geopolymer, Ye et al. (2018) and Alshaaer et al. (2017) concluded that geopolymerization causes alkaline degradation of lignin and hemicelluloses by the generation of carboxylic acids.

The degradation of the cellulose in the CAC and geopolymer pastes, indicated by the reduction of the carbon C2 on the surface of the fibers, is according to Gram (1988) and Tolêdo Filho et al. (2000). These authors have found that high alkalinity causes the hydrolysis of the cellulose molecule, leading to degradation of molecular chains and then a reduction in the degree of polymerization of the fibers.

The FTIR analysis of the pulp and NFC immersed in the different unhardened cementitious pastes also indicates the modifications that occurred in the chemical structure of the fibers due to the exposure in the alkaline environment. Hence, Figure 5 (A) and Figure 5 (B) show the spectra of pulp and NFC respectively, in the control condition and after 28 days in the unhardened pastes of the OPC, CAC and geopolymer.

The spectra display the characteristic peaks of cellulosic fibers, but it does not show clear shifts in the bands due to the exposure of the fibers under different conditions. However, the careful analysis of the OH stretching vibration peak intensities and positions within the range of 3000–3800 cm^{-1}, gives considerable information concerning the hydrogen bonds (Altaner et al. 2014; Dai and Fan 2011; Fengel 1992; 1993).

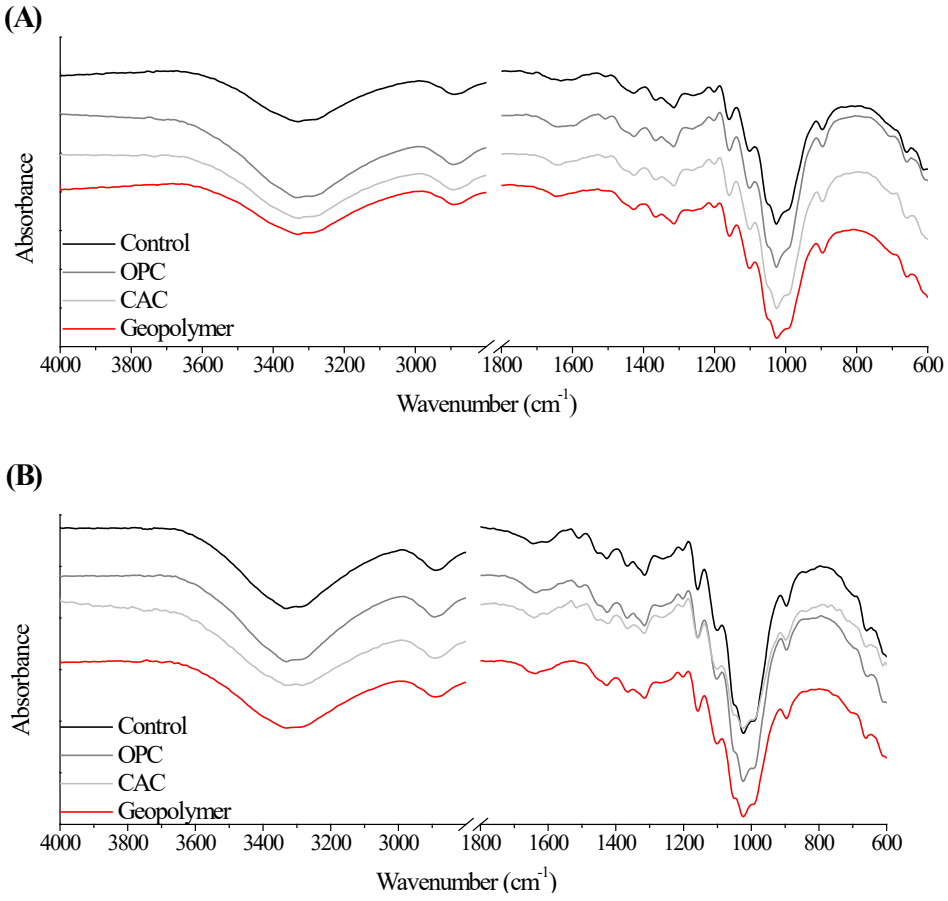

Figure 5 – FTIR spectra of pulp (A) and NFC (B) in the control condition and after 28 days of immersion in the OPC, CAC and geopolymer pastes

* The IR region between 1800 cm^{-1} and 2700 cm^{-1} has been omitted from the spectra because it does not contain any significant bands

Figure 6 and Figure 7 show the deconvoluted peaks into two bands for the curves fitting of pulp and NFC in the control condition and immersed in different unhardened cement pastes. The pulp and NFC control presented intermolecular hydrogen bonds, which are indicated in bands at 3278 cm^{-1} and at 3269 cm^{-1}, and intramolecular hydrogen bonds at 3399 cm^{-1} and at 3394 cm^{-1}, respectively. According to Zhao et al. (2019) the intramolecular hydrogen bonds for O2H…O6 and O3H…O5, and the intermolecular hydrogen bonds for O6H…O3′ in cellulose appear at 3455–

399 3410, 3375–3340, and 3310–3230 cm^{-1}, respectively, along with the valence vibration of H-
400 bonded OH groups at 3570–3450 cm^{-1}.

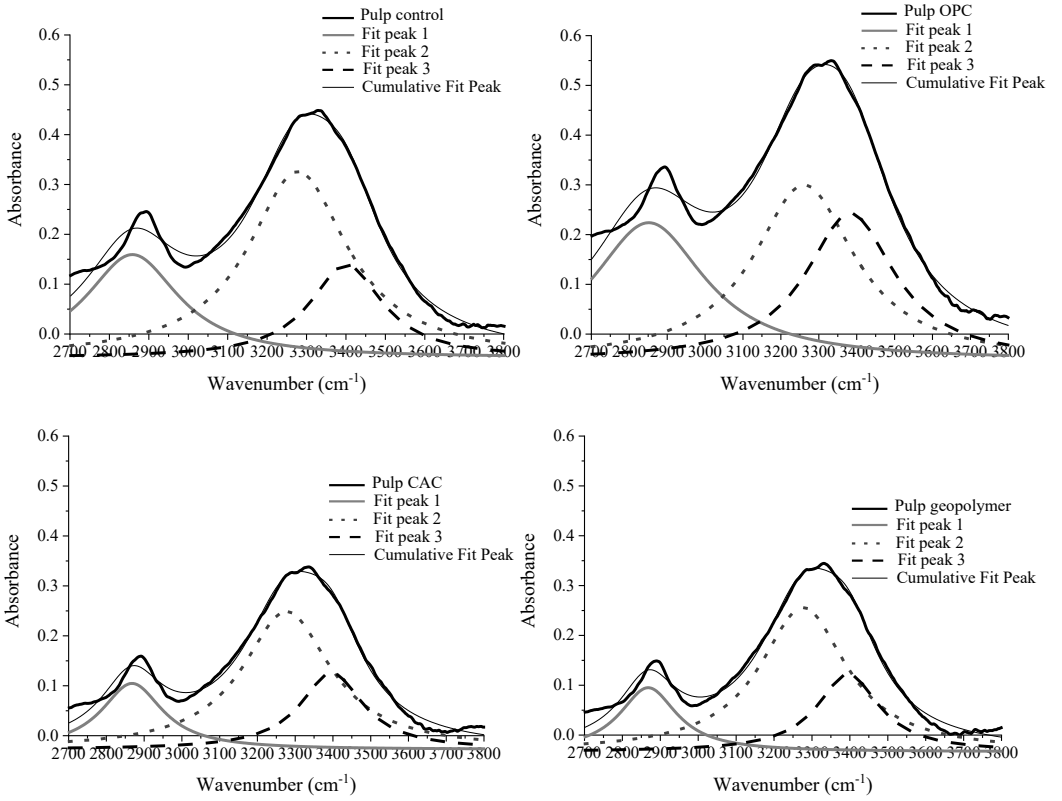

401
402

403 Figure 6 – Deconvoluted FTIR spectra of pulp control, and of pulp immersed in OPC, CAC and
404 geopolymer pastes

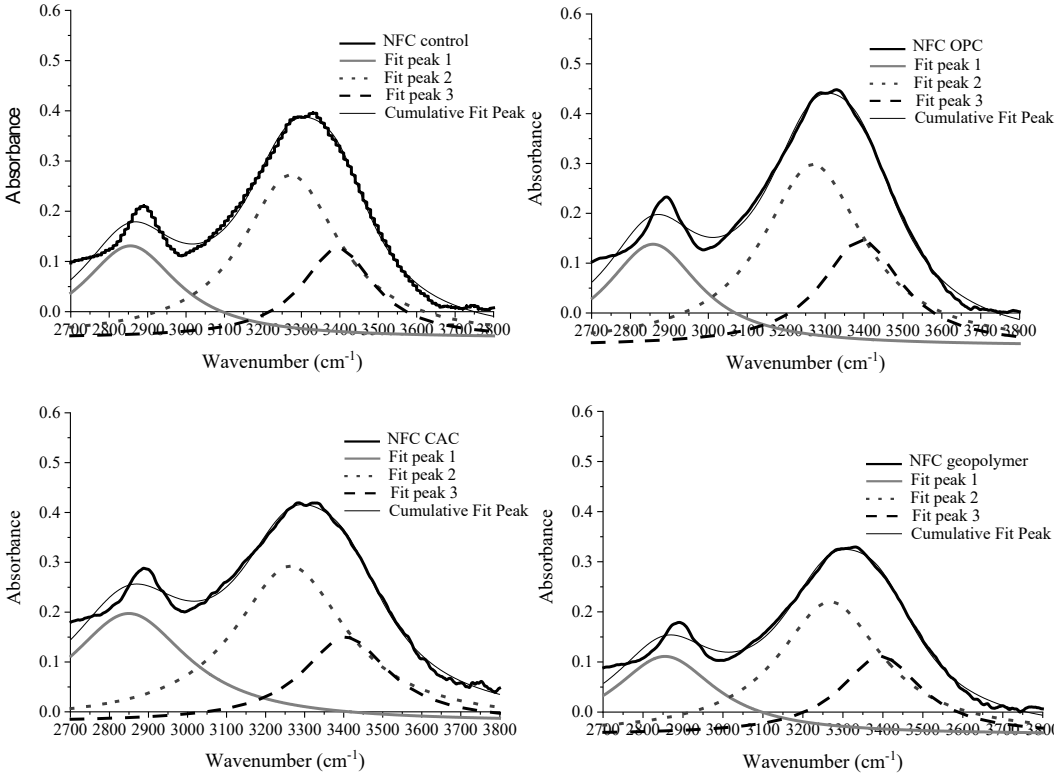

405
406

Figure 7 – Deconvoluted FTIR spectra of NFC control, and NFC immersed in OPC, CAC and geopolymer pastes

It can be seen in Figure 6, Figure 7 and Table 6 that the immersion of the fibers in the alkaline environments (OPC, CAC and geopolymer) induced in general, the slight shift of the bands to lower wave numbers (red shift), compared to the control. The exception occurred in the bands related to intramolecular hydrogen bonds of NFC CAC and NFC geopolymer, which were shifted to higher wave numbers (blue shift).

Table 6. Band positions and its hydrogen bond energy

Fibers	Band position (cm^{-1})	E_H (kJ)	Band position (cm^{-1})	E_H (kJ)
Pulp control	3278.9 ± 1.3	26.6 ± 0.1	3399.0 ± 1.2	18.0 ± 0.2
Pulp OPC	3266.7 ± 1.2	27.4 ± 0.5	3386.6 ± 0.9	18.9 ± 0.4
Pulp CAC	3272.4 ± 0.6	27.1 ± 0.1	3393.5 ± 0.8	18.4 ± 0.2
Pulp geopolymer	3275.8 ± 1.2	26.9 ± 0.1	3394.4 ± 1.7	18.4 ± 0.1
NFC control	3269.2 ± 1.6	27.4 ± 0.1	3394.5 ± 1.2	18.4 ± 0.1
NFC OPC	3271.5 ± 1.7	27.2 ± 0.2	3393.2 ± 0.8	18.5 ± 0.1
NFC CAC	3263.9 ± 0.6	27.8 ± 0.0	3404.5 ± 1.8	17.6 ± 0.1
NFC geopolymer	3266.9 ± 2.2	27.5 ± 0.2	3395.4 ± 0.4	18.3 ± 0.0

The red shift of OH stretching frequency suggest the formation of the H bond and consequently, the weakening of the OH bond, causing elongation of these OH bonds (Hobza and Havlas, 2000 and Van der Veken et al., 2001). The formation of new hydrogen bonds can be confirmed with the results of the hydrogen bonding energy, which increased with the shift of the bands to lower wave numbers frequencies.

The shift of the bands of the NFC to higher wave numbers (NFC CAC (3404 cm^{-1}) and NFC geopolymer (3395 cm^{-1})), compared to the control, gives indications of the weakening of hydrogen bond and reduction of its energy. According to Turki et al. (2018) this may be explained by the formation of new OH bonds at this frequency, but these bonds are not as strong as the initial ones due to the lack of stability and to the packing effect that makes the length of OH covalent

428 bonds shorter. These modifications, blue and red shift, indicate changes in the chemical structure
429 and hydrogen bonds of the pulp and NFC after immersion in unhardened OPC, CAC and
430 geopolymer pastes. These changes can be associated with different patterns of geometrical
431 perturbations or electron density shifts (Scheiner and Kar 2002).

432 According to Ciolacu et al. (2011) the H bonding energy is directly related to the degree
433 of crystallinity of the cellulose. Thus, the increase in H bond energy indicates changes in the
434 crystalline structure of the cellulose, ie increase in the degree of crystallinity. Therefore, the
435 increase in H bond energy indicates the degradation of the amorphous components on the surface
436 of the fibers (pulp OPC, CAC, geopolymer, and NFC OPC) after immersion in alkaline pulps. On
437 the other hand, the reduction of H bond energy of NFC CAC and NFC geopolymer is related to the
438 reduction of crystallinity, which indicates degradation of the cellulose in these fibers.

439 The immersion of the pulp and NFC in CAC, OPC and geopolymer caused slight
440 modifications in the fibers, but that were sufficient to consider the alkaline environment of these
441 pastes as being harmful during the time of exposure of lignocellulosic fibers. This is because in
442 highly alkaline environments cellulose and hemicellulose are exposed to reactions such as alkaline
443 swelling; alkaline dissolution; alkaline hydrolysis of acetyl groups; peeling-off reaction; chemical
444 and physical stopping reaction and alkaline hydrolysis (Van Loon et al. 1999; Pavasars et al.
445 2003). According to the authors, the rates at which these reactions occur are dependent on pH,
446 temperature and alkaline environment.

447 According to Nevel (1985) and Askarieh et al. (2000) at temperatures below 170 °C the
448 predominant mechanism of alkaline cellulose degradation is by a reaction that takes place at the
449 reducing end group of the chain and ruptures the 1,4-glycosidic linkage. Glucose units are
450 progressively eliminated from the reducing end of the chain, and this process is known as the
451 peeling. Terminal degradation consists of shortening of the main chain by successive elimination
452 of the terminal reducing monomer. This reaction occurs in solutions with a pH greater than 11.
453 The cellulose molecule loses about 50 to 70 units of glucose in this type of hydrolysis (Grace et
454 al., 1989).

455 According to Johansson and Samuelson (1975) the peeling reaction rate is proportional to
456 the concentration of reducing end groups of the cellulose. Sixta (2006) confirm that the alkaline
457 solubilization occurs whenever any new region containing fibers becomes accessible or when there
458 is a significant reduction in fibers size, and that the low degree of polymerization (DP) of fibers

favors the alkaline solubilization phenomenon. This indicates that the intensity of alkaline degradation is different in pulp and NFC.

The nanofibrillation process reduces considerably the DP of the fibers because the cell wall structure consisting of nanofibers in a multilayered structure and hydrogen bonds is broken down. According to Zimmermann et al. (2010) fibrillation in the laboratory led to a decrease in DP between 15% and 63%. The DP correlates with the aspect ratio of the fibrils, and this means that, shorter fibrils have a lower DP. According to Matsuoka et al. (2014) and Van Loon et al. (1999) the large number of new reducing ends is formed in cellulose during the DP reduction, and the extent of degradation depends on the number of reducing end groups, that in principle, would enable complete degradation of cellulose. In other words, the greater the number of reducing end groups, the higher the peeling reaction rate. In addition to the degree of polymerization, the higher specific surface area of NFC, which greatly increases the quantity of surface hydroxyl groups, increases the accessibility of this fiber to a greater extent of degradation.

The effect of the alkalinity of the OPC, CAC and geopolymer pastes on the mechanical strength of the pulp sheets and the NFC is complementary to the study of the chemical degradation on the surface of the fibers and can be verified in Figure 8.

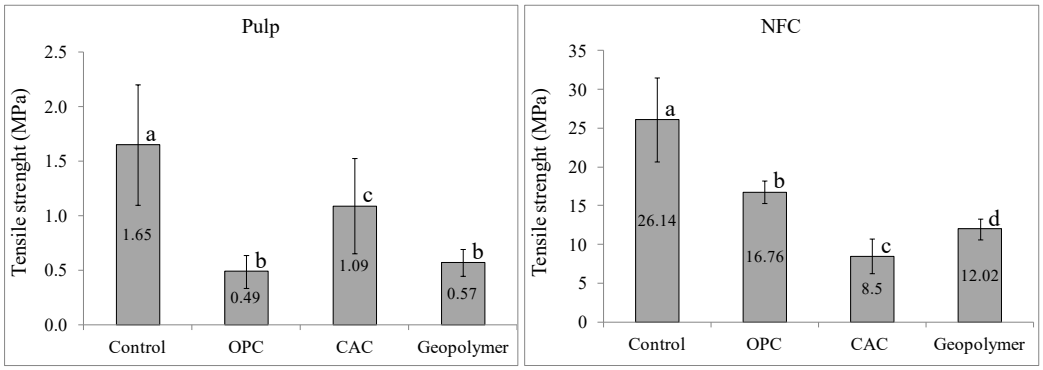

*Average values followed by the same letters do not differs significantly by the Tukey test ($p<0.05$).

Figure 8 – Tensile strength of pulp and NFC

The tensile strength results show that pulps and NFC immersed in the OPC, CAC and geopolymer pastes had statistically significant reduction in the tensile strength, in comparison to pulp and NFC control. However, the pulp immersed in CAC had the lower reduction rate (34%) in the mechanical strength after 28 days of immersion than OPC and geopolymer (approximately 70%). For the NFC the effect of the matrix was different than that found for the pulp, where the

485 lower reduction rate in the mechanical strength was to OPC (36%). The immersion of NFC in
486 CAC and geopolymer caused the higher reductions in tensile strength, which were of 68% and
487 54%, respectively.

488 As previously reported, the rate of alkaline degradation that occurs in lignocellulosic
489 fibers is directly related to pH, temperature and alkaline environment. Table 3 shows that OPC has
490 higher pH than CAC and geopolymer. However, the CAC and geopolymer pastes released more
491 heat during hydration and geopolymerization reaction, as shown in Figure 2. Thus, NFC tensile
492 strength results show that the effect of heat release on CAC hydration and geopolymer reaction
493 was more prevalent in fiber degradation than the higher pH of OPC paste. This finding can be
494 confirmed by the reduction in glycosidic bonds (C-O-C) of pulps and NFCs immersed in CAC and
495 geopolymer, which is observed by the reduction of the C2 component (Table 5).

496 Thus, this study certified that immersion of cellulosic pulp and nanofibrillated cellulose in
497 the highly alkaline and unhardened cement paste exposes them to deterioration through the
498 chemical modifications of the extractives, residual lignin and carbohydrates (cellulose and
499 hemicellulose) in the surface of the fibers.

500

501 **Conclusions**

502

503 This study showed that not only Portland cement should be considered as harmful to
504 lignocellulosic fibers, through the migration of calcium hydroxide to the lumen and cell wall of the
505 fibers. Although CAC and geopolymer are free of calcium hydroxide, the high alkalinity of these
506 matrices also accelerated the degradation process of lignocellulosic fibers.

507 The surface components of unbleached bamboo pulp and NFC, such as lignin, extractives,
508 hemicellulose and cellulose, were modified after 28 days of immersion in the alkaline cement
509 pastes. The high alkalinity of the pastes also modified the hydrogen bonds in the fibers. These
510 changes in the chemical composition and molecular structure of the fibers directly affected the
511 strength of the pulp and nanofibrillated cellulose, confirming the degradation of the fibers.

512 This study also showed that the response of the bamboo pulp and NFC immersed in the
513 high alkaline cement pastes is different due the distinctions in characteristics of these fibers. The
514 combination of factors such as, the lower degree of polymerization and high specific surface area

of NFC with the highest amount of heat released during hydration of CAC and geopolymerization favored the greatest degradation of NFC. The higher pH of OPC and the higher heat released in the first hours of geopolymer reaction may have caused the more significant changes in the chemical structure of the pulp and the reduction of its tensile strength.

Therefore, the best known means to reduce the degradation of the fibers are still those which concomitant reduce the pH and calcium hydroxide of the matrices.

Acknowledgments

The authors would like to thanks the financial support offered by São Paulo Research Foundation – FAPESP (Grants n°: 2018/00519-0; 2015/21079-0), Brazil. The authors also gratefully acknowledge Ministerio de Educación, Cultura y Deporte (Government of Spain) for financial support of this work (project BIA2014-59399-R).

References

Almeida AEFS, Tonoli GHD, Santos SF, Savastano Jr. H (2013) Improved durability of vegetable fiber reinforced cement composite subject to accelerated carbonation at early age. Cem Concr Comp 42: 49-58. http://dx.doi.org/10.1016/j.cemconcomp.2013.05.001

Alomayri T, Shaikh FUA, Low IM (2013) Characterisation of Cotton Fibre-Reinforced Geopolymer Composites. Compos Part B-Eng 50:1–6. http://dx.doi.org/10.1016/j.compositesb.2013.01.013

Alomayri T, Shaikh FUA, Low IM (2014) Synthesis and Mechanical Properties of Cotton Fabric Reinforced Geopolymer Composites. Compos Part B-Eng 60:36–42. http://dx.doi.org/10.1016/j.compositesb.2013.12.036

Alshaaer M, Mallouh SA, Al-Kafawein J et al (2017) Fabrication, Microstructural and Mechanical Characterization of Luffa Cylindrical Fibre - Reinforced Geopolymer Composite. Appl Clay Sci 143:125–133. http://dx.doi.org/10.1016/j.clay.2017.03.030

Altaner CM, Horikawa Y, Sugiyama J, Jarvis MC (2014) Cellulose Iβ investigated by IR-spectroscopy at low temperatures. Cellulose 21:3171–3179. http://dx.doi.org/10.1007/s10570-014-0360-x

Ardanuy M, Claramunt J, Arévalo R et al (2012a) Nanofibrillated Cellulose (Nfc) as a Potential Reinforcement for High Performance Cement Mortar Composites. BioResources 7(3):3883–3894

Ardanuy M, Claramunt J, Toledo Filho RD (2012b) Evaluation of Durability to Wet/Dry Cycling of Cement Mortar Composites Reinforced with Nanofibrillated Cellulose. In: Brandt AM, Glinicki MA, Olek J, Leung CKY (ed) Brittle Matrix Composites 10, 1st edn. Woodhead Publishing, Warsaw, pp 33–41

Askarieh MM, Chambers AV, Daniel FBD et al (2000) The Chemical and Microbial Degradation of Cellulose in the near Field of a Repository for Radioactive Wastes. Waste Manage 20(1):93–106. https://doi.org/10.1016/S0956-053X(99)00275-5

Assaedi H, Alomayri T, Shaikh FUA, Low IM (2015) Characterisation of Mechanical and Thermal Properties in Flax Fabric Reinforced Geopolymer Composites. J Adv Ceram 4(4):272–281. http://dx.doi.org/10.1007/s40145-015-0161-1

Bastidas JC, Venditti R, Pawlak J et al (2005) Chemical Force Microscopy of Cellulosic Fibers. Carbohydr Polym 62(4):369–378. https://doi.org/10.1016/j.carbpol.2005.08.058

Bentur A, Mindess S (2007) Fibre Reinforced Cementitious Composites, Taylor &Francis, New York

Bouafif H, Koubaa A, Perré P et al (2008) Analysis of Among-Species Variability in Wood Fiber Surface Using DRIFTS and XPS: Effects on Esterification Efficiency. J Wood Chem Technol 28(4):296–315. https://doi.org/10.1080/02773810802485139

Chakar FS, Ragauskas AJ (2004) Review of Current and Future Softwood Kraft Lignin Process Chemistry. Ind Crops Prod 20:131–141. https://doi.org/10.1016/j.indcrop.2004.04.016

Chen R, Ahmari S, Zhang L (2014) Utilization of Sweet Sorghum Fiber to Reinforce Fly Ash-Based Geopolymer. J Mater Sci 49(6):2548–2558. https://doi.org/10.1007/s10853-013-7950-0

Cheng XW, Khorami M, Shi Y, Liu KQ et al (2018) A New Approach to Improve Mechanical Properties and Durability of Low-Density Oil Well Cement Composite Reinforced by Cellulose Fibres in Microstructural Scale. Constr Build Mater 177:499–510. https://doi.org/10.1016/j.conbuildmat.2018.05.134

Ciolacu D, Ciolacu F, Popa VI (2011) Amorphous Cellulose – Structure and Characterization. Cellulose Chem Technol 45(12):13–21.

Claramunt J, Fernandez-Carrasco L, Ardanuy M (2018) Mechanical Performance of Flax Nonwoven-Calcium Aluminate Cement Composites. In: Mechtcherine V, Slowik V, Kabele P (eds) Strain-Hardening Cement-Based Composites: SHCC4. RILEM Bookseries 15. Springer Netherlands, Heidelberg, pp 375-382

Coutts RSP, Ni Y (1995) Autoclaved Bamboo Pulp Fibre Reinforced Cement. Cem Concr Comp 17(2):99–106. https://doi.org/10.1016/0958-9465(94)00002-G

Correia VC, Santos V, Sain M, Santos SF, Leão AL, Savastano Jr. H (2016) Grinding process for the production of nanofibrillated cellulose based on unbleached and bleached bamboo organosolv pulp. Cellulose 23 (5): 2971 - 2987. https://doi.org/10.1007/s10570-016-0996-9

Correia VC, Santos SF, Mármol G, Curvelo AAS, Savastano Jr. H (2014) Potential of Bamboo Organosolv Pulp as a Reinforcing Element in Fiber-Cement Materials. Constr Build Mater 72:65-71. https://doi.org/10.1016/j.conbuildmat.2014.09.005

Correia VC, Santos SF, Teixeira RS, Savastano Jr. H (2018a) Nanofibrillated Cellulose and Cellulosic Pulp for Reinforcement of the Extruded Cement Based Materials. Constr Build Mater 160:376–384. https://doi.org/10.1016/j.conbuildmat.2017.11.066

Correia VC, Santos SF, Savastano Jr. H, John VM (2018b) Utilization of Vegetable Fibers for Production of Reinforced Cementitious Materials. RILEM Tech Lett 2:145-154. https://doi.org/10.21809/rilemtechlett.2017.48

Dai D, Fan M (2011) Investigation of the Dislocation of Natural Fibres by Fourier-Transform Infrared Spectroscopy. Vib Spectrosc 55(2):300–306. http://dx.doi.org/10.1016/j.vibspec.2010.12.009

European Committee for Standardization. EN 197-1:201: Cement - Part 1: Composition, specifications and conformity criteria for common cements, Brussels, 2011.

British Standards Institution. BS EN 14647:2005: Calcium aluminate cement. Composition, specifications and conformity criteria, London, 2005.

Fengel D (1992) Characterization of Cellulose by Deconvoluting the OH Valency Range In FTIR Spectra. Holzforschung 46(4):283–288. https://doi.org/10.1515/hfsg.1992.46.4.283

Fengel D (1993) Influence of Water on the OH Valency Range in Deconvoluted FTIR Spectra of Cellulose. Holzforschung 47(2):103–108. https://doi.org/10.1515/hfsg.1993.47.2.103

Firdous R, Stephan D, Djobo JNY (2018) Natural Pozzolan Based Geopolymers: A Review on Mechanical, Microstructural and Durability Characteristics. Constr Build Mater 190:1251–1263. https://doi.org/10.1016/j.conbuildmat.2018.09.191

Fuentes CA, Tran LQN, Van Hellemont M, Janssens V, (2013) Effect of Physical Adhesion on Mechanical Behaviour of Bamboo Fibre Reinforced Thermoplastic Composites. Colloids Surf A Physicochem Eng Asp 418:7–15. http://dx.doi.org/10.1016/j.colsurfa.2012.11.018

George M, Mussone PG, Bressler DC (2015) Modification of the Cellulosic Component of Hemp Fibers Using Sulfonic Acid Derivatives: Surface and Thermal Characterization. Carbohydr Polym 134:230–239. http://dx.doi.org/10.1016/j.carbpol.2015.07.096

Grace TM, Leopold B, Malcolm EW (1989) Chemical reactions of wood constituents. In: Grace TM, Leopold B, Malcolm EW (ed) Pulp and paper manufacture: Alkaline pulping, vol 5. 3rd edn. TAPPI, Atlanta, pp 23-44.

Gram HE (1988) Natural Fibre Concrete Roofing. In: Swamy RN (ed) Natural fibre reinforced cement and concrete, vol 5. Blackie and Son Ltd, London, pp 256-285.

Hermansson K (2002) Blue-Shifting Hydrogen Bonds. J Phys Chem A 106(18):4695–4702. https://doi.org/10.1021/jp0143948

Hobza P, Havlas Z (2000) Blue-Shifting Hydrogen Bonds. Chem Rev 100 (11): 4253−4264. https://doi.org/10.1021/cr990050q

Holmberg M, Berg J, Stemme S et al (1997) Surface Force Studies of Langmuir-Blodgett Cellulose Films. J Colloid Interf Sci 186(2):369–381. https://doi.org/10.1006/jcis.1996.4657

Hua X, Kaliaguine S, Kokta BV, Adnot A (1993) Surface Analysis of Explosion Pulps by ESCA Part 1. Carbon (1s) Spectra and Oxygen-to-Carbon Ratios. Wood Sci Technol 27(6):449–459. http://link.springer.com/10.1007/BF00193868

Johansson MH, Samuelson O (1975) End-wise Degradation of Hydrocellulose during Hot Alkali Treatment. J Appl Polym Sci 19(11):3007–3013. https://doi.org/10.1002/app.1975.070191106

Johansson LS (2002) Monitoring Fibre Surfaces with XPS in Papermaking Processes. Microchim Acta 138:217–223. https://doi.org/10.1007/s006040200025

Johansson LS, Campbell JM, Fardim P, Hultén AH et al (2005) An XPS Round Robin Investigation on Analysis of Wood Pulp Fibres and Filter Paper. Surf Sci 584(1):126–132. https://doi.org/10.1016/j.susc.2005.01.062

Khale D, Chaudhary R (2007) Mechanism of Geopolymerization and Factors Influencing Its Development: A Review. J Mater Sci 42(3):729–746. https://doi.org/10.1007/s10853-006-0401-4

Klemm D, Craston ED, Fisher D, Gama M, et al (2018) Nanocellulose as a Natural Source for Groundbreaking Applications in Materials Science : Today ' s State. Mater Today 21(7):720–748. https://doi.org/10.1016/j.mattod.2018.02.001

Klemm D, Kramer F, Moritz S, Lindström T et al (2011) Nanocelluloses : A New Family of Nature-Based Materials. Angew Chem Int Ed 50(24): 5438–5466. https://doi.org/0.1002/anie.201001273

Laine J, Stenius P, Carlsson G, Strom G (1994) Surface characterization of unbleached kraft pulps by means of ESCA. Cellulose 1(2):145–160. https://doi.org/10.1007/BF00819664

Li M, Zhou S, Guo X (2017) Effects of Alkali-Treated Bamboo Fibers on the Morphology and Mechanical Properties of Oil Well Cement. Constr Build Mater 150:619–625. http://dx.doi.org/10.1016/j.conbuildmat.2017.05.215

Mármol G, Savastano Jr. H (2017) Study of the Degradation of Non-Conventional MgO-SiO2cement Reinforced with Lignocellulosic Fibers. Cem Concr Comp 80:258–267. https://doi.org/10.1016/j.cemconcomp.2017.03.015

Matsuoka S, Kawamoto H, Saka S (2014) What Is Active Cellulose in Pyrolysis? An Approach Based on Reactivity of Cellulose Reducing End. J Anal Appl Pyrol 106:138–146. https://doi.org/10.1016/j.jaap.2014.01.011

Migneault S, Koubaa A, Perré P, Riedl B (2015) Effects of Wood Fiber Surface Chemistry on Strength of Wood-Plastic Composites. Appl Surf Sci 343:11–18. http://dx.doi.org/10.1016/j.apsusc.2015.03.010

Missoum K, Belgacem MN, Bras J (2013) Nanofibrillated Cellulose Surface Modification: A Review. Materials 6(5):1745–1766. http://dx.doi.org/10.3390/ma6051745

Mohr BJ, Biernacki JJ, Kurtis KE (2006) Microstructural and Chemical Effects of Wet/Dry Cycling on Pulp Fiber-Cement Composites. Cem Concr Res 36(7):1240–1251. https://doi.org/10.1016/j.cemconres.2006.03.020

Mohr BJ, Biernacki JJ, Kurtis KE (2007) Supplementary Cementitious Materials for Mitigating Degradation of Kraft Pulp Fiber-Cement Composites. Cem Concr Res 37(11):1531–1543. https://doi.org/10.1016/j.cemconres.2007.08.001

Mohr BJ, Nanko H, Kurtis KE (2005a) Durability of Kraft Pulp Fiber-Cement Composites to Wet/Dry Cycling. Cem Concr Comp 27(4):435–448. https://doi.org/10.1016/j.cemconcomp.2004.07.006

Mohr BJ, Nanko H, Kurtis KE (2005b) Durability of Thermomechanical Pulp Fiber-Cement Composites to Wet/Dry Cycling. Cem Concr Res 35(8):1646–1649. https://doi.org/10.1016/j.cemconres.2005.04.005

Nevell TP (1985) Degradation of cellulose by acids, alkalis, and mechanical means, In: Nevell TP, Zeronian SH, (ed) Cellulose chemistry and its applications. Ellis Horwood, Hemel Hempstead, pp. 223-242.

Pavasars I, Hagberg J, Borén H, Allard B (2003) Alkaline Degradation of Cellulose: Mechanisms and Kinetics. J Polym Environ 11(2): 39–47. https://doi.org/10.1023/A:102426770

Poletto M, Ornaghi HL, Zattera AJ (2014) Native Cellulose: Structure, Characterization and Thermal Properties. Materials 7(9): 6105–6119. https://doi.org/10.3390/ma7096105

Popescu CM, Dobele G, Rossinskaja G, Dizhbite T, Vasile C (2007) Degradation of Lime Wood Painting Supports. Evaluation of Changes in the Structure of Aged Lime Wood by Different Physico-Chemical Methods. J Anal Appl Pyrolysis 79(1–2):71–77. https://doi.org/10.1016/j.jaap.2006.12.014

Rodrigues CS, Ghavami K, Stroeven P (2006) Porosity and Water Permeability of Rice Husk Ash-Blended Cement Composites Reinforced with Bamboo Pulp. J Mater Sci 41(21):6925–6937. https://doi.org/10.1007/s10853-006-0217-2

741 Rodrigues CS, Ghavami K, Stroeven P (2010) Rice Husk Ash as a Supplementary Raw Material
742 for the Production of Cellulose-Cement Composites with Improved Performance. Waste Biomass
743 Valorization 1(2):241–249. https://doi.org/10.1007/s12649-010-9017-7
744
745 Santos SF, Schmidt R, Almeida AEFS, Tonoli GHD, Savastano Jr. H (2015) Supercritical
746 Carbonation Treatment on Extruded Fibre-Cement Reinforced with Vegetable Fibres. Cem Concr
747 Comp 56:84–94. https://doi.org/10.1016/j.cemconcomp.2014.11.007
748
749 Scheiner S, Tapas K (2002) Red- versus Blue-Shifting Hydrogen Bonds: Are There Fundamental
750 Distinctions? J Phys Chem A 106(9):1784–1789. https://doi.org/10.1021/jp013702z
751
752 Šiler P, Kolářová I, Sehnal T, Másilko J, Opravil T (2016) The Determination of the Influence of
753 PH Value of Curing Conditions on Portland Cement Hydration. Procedia Eng 151:10–17.
754 https://doi.org/10.1016/j.proeng.2016.07.393
755
756 Singh SM (1985) Alkali Resistance of Some Vegetable Fibers and Their Adhesion with Portland
757 Cement. Res Ind 15: 121-126.
758
759 Sixta H (2006) Handbook of pulp, 1st edn. Wiley-VCH, Weinheim
760
761 Tailby J, MacKenzie KJD (2010) Structure and Mechanical Properties of Aluminosilicate
762 Geopolymer Composites with Portland Cement and Its Constituent Minerals. Cem Concr Res
763 40(5):787–794. http://dx.doi.org/10.1016/j.cemconres.2009.12.003
764
765 Tolêdo Filho RD, Scrivener K, England GL, Ghavami K (2000) Durability of Alkali-Sensitive
766 Sisal and Coconut Fibres in Cement Mortar Composites. Cem Concr Comp 22(2):127–143.
767 https://doi.org/10.1016/S0958-9465(99)00039-6
768
769 Tolêdo Filho RD, Ghavami K, England GL, Scrivener K (2003) Development of Vegetable Fibre-
770 Mortar Composites of Improved Durability. Cem Concr Comp 25(2):185–196.
771 https://doi.org/10.1016/S0958-9465(02)00018-5
772
773 Turki A, Oudiani AE, Msahli S, Sakli F (2018) Investigation of OH Bond Energy for Chemically
774 Treated Alfa Fibers. Carbohydr Polym 186:226–235.
775 https://doi.org/10.1016/j.carbpol.2018.01.030
776
777 Van der Veken BJ, Herrebout WA, Szostak R et al (2001) The Nature of Improper, Blue-Shifting
778 Hydrogen Bonding Verified Experimentally. J Am Chem Soc 123(49):12290–12293.
779 https://doi.org/10.1021/ja010915t
780
781 Van Loon LR, Glaus MA, Laube A, Stallone S (1999) Degradation of Cellulosic Materials under
782 the Alkaline Conditions of a Cementitious Repository for Low- and Intermediate Level
783 Radioactive Waste. Part III: Effect of Degradation Products on the Sorption of Radionuclides on
784 Feldspar. Radiochim Acta 86(3-4):183-190. https://doi.org/10.1524/ract.1999.86.34.183
785
786 Villa C, Pecina ET, Torres R, Gómez L (2010) Geopolymer Synthesis Using Alkaline Activation
787 of Natural Zeolite. Constr Build Mater 24(11):2084–2090.
788 http://dx.doi.org/10.1016/j.conbuildmat.2010.04.052
789
790 Wei J (2018) Degradation Behavior and Kinetics of Sisal Fiber in Pore Solutions of Sustainable
791 Cementitious Composite Containing Metakaolin. Polym Degrad Stab 150:1–12.
792 https://doi.org/10.1016/j.polymdegradstab.2018.01.027
793
794 Wei J, Meyer C (2015) Degradation Mechanisms of Natural Fiber in the Matrix of Cement
795 Composites. Cem Concr Res 73:1–16. http://dx.doi.org/10.1016/j.cemconres.2015.02.019
796
797 Wei J, Meyer C (2017) Degradation of Natural Fiber in Ternary Blended Cement Composites
798 Containing Metakaolin and Montmorillonite. Corros Sci 120:42–60.
799 http://dx.doi.org/10.1016/j.corsci.2016.12.004
800

Xie X, Zhou Z, Jiang M, Xu X, Wang Z, Hui D (2015) Cellulosic Fibers from Rice Straw and Bamboo Used as Reinforcement of Cement-Based Composites for Remarkably Improving Mechanical Properties. Compos Part B-Eng 78:153–161. http://dx.doi.org/10.1016/j.compositesb.2015.03.086

Yan L, Kasal B, Huang L (2016) A Review of Recent Research on the Use of Cellulosic Fibres, Their Fibre Fabric Reinforced Cementitious, Geo-Polymer and Polymer Composites in Civil Engineering. Compos Part B-Eng 92:94–132. http://dx.doi.org/10.1016/j.compositesb.2016.02.002

Ye H, Zhang Y, Yu Z, Mu J (2018) Effects of Cellulose, Hemicellulose, and Lignin on the Morphology and Mechanical Properties of Metakaolin-Based Geopolymer. Constr Build Mater 173:10–16. https://doi.org/10.1016/j.conbuildmat.2018.04.028

Zhao D, Deng Y, Han D, Tan L, Ding Y et al (2019) Exploring Structural Variations of Hydrogen-Bonding Patterns in Cellulose during Mechanical Pulp Refining of Tobacco Stems. Carbohydr Polym 204:247–254. https://doi.org/10.1016/j.carbpol.2018.10.024

Zimmermann T, Bordeanu N, Strub E (2010) Properties of Nanofibrillated Cellulose from Different Raw Materials and Its Reinforcement Potential. Carbohydr Polym 79(4):1086–1093. https://doi.org/10.1016/j.carbpol.2009.10.045